

# Generating Infinite-Size Textures using GANs with Patch-by-Patch Paradigm

Alhasan Abdellatif <sup>\*1</sup> and Ahmed H. Elsheikh <sup>†1</sup>

<sup>1</sup>Heriot-Watt University

December 12, 2023

## Abstract

In this paper, we introduce a novel approach for generating texture images of infinite sizes using Generative Adversarial Networks (GANs) based on a patch-by-patch paradigm. Existing texture synthesis techniques rely on generating large-scale textures using a single forward pass to the generative model; this approach limits the scalability and flexibility of the images produced. In contrast, the proposed approach trains a GAN model on a single texture image to generate relatively small-size patches that are locally correlated and can be seamlessly concatenated to form a larger image. The method relies on local padding in the generator to ensure consistency between the generated patches. It also utilizes spatial stochastic modulation to allow for local variations and improve patterns alignment in the large-scale image. The trained models learn the local texture structure and are able to generate images of arbitrary sizes, while also maintaining the coherence and diversity. Experimental results demonstrate constant GPU scalability with respect to the generated image size compared to existing approaches that exhibit a proportional growth in GPU memory.

**Keywords:** Generative Adversarial Networks (GANs), Texture Synthesis.

## 1 Introduction

Texture synthesis refers to the process of generating arbitrary-size textures that are visually similar to a given input example, while also being diverse and not a simple duplication of the input image. This problem has numerous applications in fields such as gaming, virtual reality and graphic design, where high-quality textures are critical for creating realistic and visually appealing environments.

---

<sup>\*</sup>aa519@hw.ac.uk

<sup>†</sup>a.elsheikh@hw.ac.uk

Classical approaches to texture synthesis [1, 2] were based on statistical modelling and Markov random fields, while more recent methods leverage deep learning techniques to generate high-quality textures with more complex structures and fine-grained details.

The use of Generative Adversarial Networks (GANs) [3] in generating high-quality images has been widely researched [4–8]. Moreover, the potential of using GANs for generating realistic textures has also been explored. Several methods have been proposed for this task, including Spatial GAN [9], PSGAN [10], and adversarial expansion [11]. However, these methods fail to generate infinite-size or relatively large-scale textures due to scalability limitations in memory with respect to the output image size. Studies such as [4, 5, 12, 13] were able to train GANs to generate images of large sizes. However, generating images of arbitrary size is not directly possible with these models, as they are trained on images of finite resolutions, and training on extremely large sizes is constrained by limited resources.

The patch-by-patch generation approach generates images by assembling correlated patches together to form a larger image, which allows for infinite resolution and avoids training instabilities. Recent studies have extended this approach to generate natural images, utilizing coordinate-conditioning [14], padding-free generators [15], and spatially-equivariant generators [16]. However, generating stationary texture images with this approach does not require explicit coordinates due to their self-similarity and homogeneity. It is sufficient to capture the local spatial structure of the texture and produce locally correlated patches independently. Nonetheless, training these models on a single texture image is challenging due to their reliance on a large number of training samples.

In this paper, we developed a novel GAN architecture to synthesize stationary textures of infinite sizes based on patch-by-patch generation trained on a single texture image. Our approach uses *local padding*, instead of zero-padding, where the input and the generator feature maps are padded with content from neighbouring patches ensuring seamless concatenation. In addition, we use *spatial stochastic modulation*, where the generator activations are modulated spatially using stochastic maps; this allows for local variations and improves alignment for texture images that exhibit global characteristics. By incorporating both *local padding* and *spatial stochastic modulation* techniques, the model demonstrated its capability to generate patches that can be seamlessly concatenated to form a larger image. Furthermore, the proposed approach offers a scalable solution for generating texture images at very large sizes, provided only a single training image.

The rest of the paper is organized as follows: in the next section we review related work. In section 3, we discuss the new developed patch-by-patch approach. In section 4, we show and discuss the results. Finally, a conclusion is given in section 5.

## 2 Related Work

### 2.1 Generative Adversarial Networks (GANs)

Generative Adversarial Networks (GANs) [3] are deep learning models that have gained significant attention in recent years due to their ability to generate realistic images. The development of GANs has been an active area of research, with various modifications and improvements proposed to address issues such as instability during training, mode collapse and the difficulty of generating high-resolution images [4, 5, 17–20]. GANs have found numerous applications in computer vision, ranging from image-to-image translation [6], super-resolution [7], and image in-painting [8].

### 2.2 Texture Generation Using GANs

Generative Adversarial Networks (GANs) have shown great potential in generating high-quality images, but they can also be used to generate realistic textures. One of the challenges in texture generation is to generate samples with high visual quality while preserving the coherence and consistency of the texture. Spatial GAN [9] builds upon the traditional GANs architecture by transforming the generator and discriminator into fully convolutional networks. In this way, a spatial input is mapped into an output texture image which can be expanded in size by expanding the input. Periodic Spatial GAN (PSGAN) [10] is an extension of Spatial GAN proposed to generate textures with periodic patterns where they incorporated a periodic input into the generator network to ensure that the generated textures have a periodic structure. The work by [11] has used adversarial expansion to double the size of the input texture image. In [21], a GANs-based architecture for generating realistic images from a single input image was introduced and used to generate images of texture of high resolution.

The main drawback of these methods is the scalability in memory, i.e., increasing the size of the output image will increase the required GPU memory, this hinders the infinite size generation. Moreover, [11] did not parametrize the stochasticity of the texture, instead they performed diversification by shuffling and cropping. LocoGAN [22] trains a fully convolutional GANs on sub-images instead of the full image and uses coordinates to inform the model which part of the image is being generated. To generate texture images, they used periodic coordinates which allowed the model to generate periodic texture that lacks diversity and randomness.

TileGAN [23] was able to generate texture of hundreds of megapixels; however, it focuses on a different task where the aim was to combine different patches generated by GANs by passing the pre-stored latent tiles to the trained generator. This requires searching for the closest latents using a neighbourhood similarity match which is not a scalable and deployable solution.

### 2.3 Patch-by-patch Generation

In the patch-by-patch generation paradigm, the generator synthesizes one small patch at a time then correlated patches are assembled to form a larger image. This allows the model to generate images with infinite sizes and avoid the problem of limited resources. In addition, this patch-based approach has avoided the training instabilities that occur when generating a large image in a single forward pass through the generator as noted in [5]. In [14], they trained a GAN model that conditions image patches on coordinates and then assembled patches that share a global vector together. This approach allowed for limited extrapolation of the images by extending the coordinates. It also facilitated the generation of panoramas using cylindrical coordinates.

The work in [15] extended the method to natural images by employing a padding-free generator. This approach removed zero-padding in convolutional neural networks and instead they padded the inputs with neighbouring content, allowing for seamless concatenation. Additionally, they utilized an implicit neural function with CoordConv [24], where the hidden representations are concatenated with positional embeddings. These embeddings encode the coordinates, providing positional information for each patch.

In [16], they used a spatially-equivariant generator where they modified the AdaIN algorithm [25] such that the modulating parameters are spatially-interpolated and they also used CoordConv [24]. This approach enabled the generation and assembly of vertical patches of natural scenes. However, the model suffers from content repetition when the global anchors do not change fast enough to allow for variations. In addition, the padding used in the generation led to blocky artefacts and discontinuity between the generated patches.

These methods are mainly trained for complex scene generation such as natural images or faces. However, unlike natural images that require global coordination between their different parts, generating stationary texture images with the patch-by-patch paradigm does not require explicit coordinates. This is due to the self-similarity and homogeneity of the texture images. Thus, the texture generative model could capture the local spatial structure of the texture and produce locally correlated patches independently without the need for explicit coordination between them. Moreover, while these methods have demonstrated success in generating natural scenes, training them on a single texture image is challenging due to their reliance on a large number of training samples.

### 2.4 Conditional Normalization

Conditional Instance Normalization (CIN) [26] is a conditional normalization technique that extends Instance Normalization (IN) [27] to enable conditional generation of images. CIN involves scaling and shifting the features in each feature map based on a given condition, such as a style vector. AdaIN [25], on the other hand, learns the scaling and shifting from an input image enabling style transfer from images. In [28], they introduced spatially-adaptive normalization (SPADE) at multiple scales of the generator network to allow a semantic

map to spatially modulate the generated image. Specifically, SPADE spatially modulates the affine parameters (i.e., scaling and shifting parameters) of the normalization layer using the semantic input image. As a consequence, one can use the spatial modulation to modify (i.e., modulate) a part of the image while keeping the rest of the image consistent.

### 3 Methodology

The proposed method relies on locality of information within the texture images. This property allows us to synthesize texture patches using only the information from the neighbouring patches. In contrast, complex scenes such as natural images and human faces do not exhibit this high degree of locality or self-similarity. The patterns in these scenes are more varied and irregular, and the relationships between local patches are not as predictable. As a result, synthesizing larger patches in complex scenes from smaller ones requires long-range interactions, i.e., sharing information between all patches in the image, as well as coordinating between patches, such as the methods developed in [14–16].

The proposed method is built on top of the SPADE [28] architecture with modifications in the generator and the training methodology. We modified the generator to be a fully convolutional generator similar to [9, 10] and removed all zero-padding following [15]. However, instead of expanding the spatial noise  $z$  to generate larger images, we limit the generator to synthesize  $N \times N$  small-size patches, each patch is of size  $h \times w$ . The patches are synthesized in parallel and can be seamlessly assembled together to form a larger image of size  $Nh \times Nw$ . The assembling is done by indexing each patch and concatenating these patches into one image based on that index. In our implementation, we set  $N = 3$ , with each patch being either  $64 \times 64$  or  $128 \times 128$  in size for larger texture images.

An overview of the method is presented in figure 1. The generator  $G$  generates a patch  $x_i = G(z_i, M_i, p_{l,i})$ . The first input is a spatial noise  $z_i$  serves as a starting input to the generator. The second input is a *stochastic spatial map*  $M_i$ , which is a 2D input that spatially modulates the feature channels of each patch. This map allows for local variations in the generated images and ensures that alignment is preserved for textures that exhibit long-range characteristics. The third input is *local padding*  $p_{l,i}$ , which pads the inputs (both  $z_i$  and  $M_i$ ) and the feature maps of each layer in the generator with content from neighbouring patches instead of the conventional zero-padding, this helps to ensure that the generated patch has consistent and smooth transitions between its neighbouring patches. In the following subsections, we explain the *local padding* and the *stochastic spatial modulation* (SSM).

The assembled image, denoted as  $X = F(x_1, x_2, \dots, x_{N^2})$ , where  $F$  is a simple concatenation function, is passed to a PatchGAN discriminator [28, 29]. This discriminator, with no additional conditions, evaluates the quality of individual image patches rather than the entire image. The PatchGAN discriminator is designed to provide a more fine-grained evaluation of the generated images, particularly for high-resolution images, by focusing on the local features of the

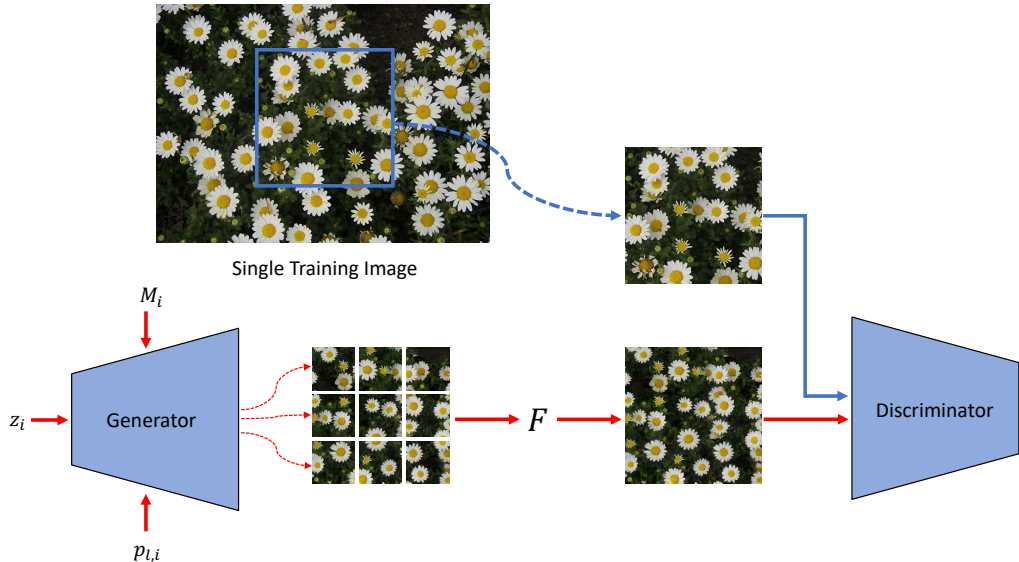


Figure 1: Overview of the training process for the proposed method. An image patch is cropped randomly from the single texture image and is passed to the discriminator. The generator takes 3 different inputs: starting input  $z_i$ , modulation map  $M_i$  and local padding  $p_{l,i}$  to generate 9 small-size patches  $x_i = G(z_i, M_i, p_{l,i}) \forall i \in 1 \dots 9$  that are passed to an assembling function  $F$  to form a larger image  $X = F(x_1, x_2, \dots, x_9)$  which is then passed to the discriminator. The blue arrows indicate the real patches path while the red arrows indicate the generated patches path. Both the generator and discriminator are fully convolutional neural networks.

image rather than the global features. Similar to [10], we removed the normalization layers in the PatchGAN discriminator and found this to be more stable and boosted performance when training on a single image. In the meantime, multiple patches of fixed size  $h_r \times w_r$  are randomly cropped from the single texture image. These real patches are passed to the PatchGAN discriminator for evaluation. Subsequently, the generator uses this feedback to adjust its weights, thereby generating new patches that better match the real ones and can also be smoothly joined together.

### 3.1 Local Padding

We introduce *local padding* as a type of padding used in convolutional neural networks (CNNs), where the inputs and features of each level are padded by the content of neighbouring patches. Typically, padding involves adding extra rows and columns of zeros around the input image or feature map to ensure that the

convolutional filters can be applied to the edges of the image or feature map. However, using zero-padding in a patch-by-patch generator results in visible seams between the concatenated patches. This mismatch occurs because the pixels in the zero-padding may not align perfectly with those in the neighbouring patches. Consequently, this results in visible differences in colour or texture at the seam.

Local padding, on the other hand, tries to address this issue by using the generated content of neighbouring patches to fill in the padded regions. Instead of padding with zeros, local padding uses the values from the input or the feature maps of adjacent patches to fill in the padded pixels, as depicted in figure 2. This ensures that the convolutional filters can be applied to the edges of the feature map without losing information and without introducing seam artefacts when concatenating patches together. Local padding can be applied to different levels, such as the input level or intermediate levels. The amount of padding applied at each level depends on the size and the number of the convolutional filters used. In our approach, we perform local padding to all inputs  $z$  and  $M$  as well as to the feature maps of the generator layers before applying the convolutional operators. This ensures that the neighbouring context is provided to all levels when generating the local patch.

The values used for padding are obtained from the neighbouring patches synthesized in parallel, (e.g., the  $3 \times 3$  patches in figure 1). For the outer patches, we use replicate padding to extend the maps along the edges, as we do not have neighbouring patches to provide padding values. This results in joint generation of the  $3 \times 3$  patches as the padding values are exchanged along the seams during the generation process. Consequently, all the 9 patches must fit within the GPU memory. However, this approach lends itself to an easy extension to infinite image generation as we will detail later in subsection 3.3. Although other combinations are possible,  $3 \times 3$  is used as it is the simplest combination that the generator needs to learn the local information between patches (i.e., 1 central and 8 neighbouring patches).

In our architecture, since we use  $3 \times 3$  convolution, we pad the input  $z$  by 1 value from neighbouring patches before mapping it using a single convolutional layer. For the stochastic modulating map, we pad with 2 values, since we pass it to 2 successive convolutional layers. For example, at the  $4 \times 4$  level, we pad the  $4 \times 4$  map with values from the maps of neighbouring patches resulting in an input map of size  $8 \times 8$ . At all intermediate levels, we pad the input to each convolutional operator with 1 value from the padding context generated in parallel.

## 3.2 Stochastic Spatial Modulation (SSM)

*Spatial stochastic modulation (SSM)* is a modified version of the Spatially-Adaptive De-normalization (SPADE) algorithm [28], which is an image-to-image translation method for synthesizing images based on semantic maps that provide information on the class and location of objects in the image. SPADE allows for spatial control on the generated images (i.e., locally modifying part

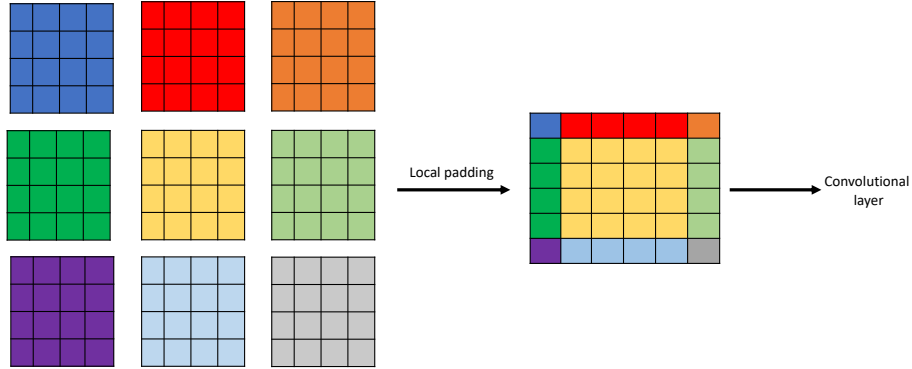


Figure 2: Local padding applied to an input, of size  $4 \times 4$ , of a convolutional layer. The features of neighbouring patches are used to pad the central patch (yellow) and the result are then passed to a convolutional layer. Unlike zero-padding where the input is simply padded with zero values, local padding gives positional context to the central patch. The same process is applied to all patches, except for the border pixels in the outer patches where replicate padding is used as there is no neighbouring content.

of the semantic map will modify the corresponding part in the generated image and keep the rest of the image consistent).

In SSM, we replaced the semantic map with a stochastic map, which allows for a greater degree of randomness. This stochasticity enhances the diversity and variability of the synthesized textures, allowing for a more realistic and natural appearance. Moreover, in cases where textures exhibit long-range alignments (e.g., bricks), fixing the  $z$  vector for all patches within the image, and making the stochastic map  $M$  the primary source of randomness ensure that the resulting textures exhibit the desired level of local variations while still adhering to the global alignment embedded in the latent vector  $z$ .

The stochastic map  $M$  is sampled from a standard normal distribution independently for each layer in the generator. This noise is then processed by two convolutional layers with the aforementioned local padding using shared information between the small patches, separated by a ReLU activation function similar to the original method. The output spatial parameters  $\gamma$  and  $\beta$  are then used to modulate the normalized activations in the generator network with the following equation:

$$\hat{h}_{k,c,x,y}(M) = \gamma_{k,c,x,y}(M) \frac{h_{k,c,x,y} - \mu_{k,c}}{\sigma_{k,c}} + \beta_{k,c,x,y}(M), \quad M \in \mathbb{R}^{H \times W}, \quad (1)$$

where  $h_{k,c,x,y}$  is the activation of the  $k^{\text{th}}$  layer and channel  $c$  at position



$x$  and  $y$  and  $\mu_{k,c}$  and  $\sigma_{k,c}$  are mean and standard deviation of the activations calculated across the batch instances and all positions.

### 3.3 Scaling to Infinite Sizes

By using the described techniques, we can generate a larger image  $X_j$ , which is a concatenation of several  $x_i$ , of size  $Nh \times Nw$  that is visually consistent. The scaling process in the horizontal direction is explained in figure 3, where  $N = 3$  and  $h = w = 128$ . First, the same process is repeated to generate a new image  $X_{j+1}$  of the same size  $Nh \times Nw$ . However, the rightmost patches in  $X_j$ , which were generated using replicate padding, will now be regenerated in  $X_{j+1}$  using local padding, i.e., using values from neighbouring patches which provide accurate padding information, ensuring visual consistency between the generated patches in both images. The rightmost patches in  $X_j$  are then dropped and the remaining patches are concatenated with the patches in  $X_{j+1}$  to form a new image  $X_{j,j+1}$  of size  $Nh \times (2N - 1)w$ .

Figure 3 shows that the left side of leftmost patches  $X_2$  are very similar to the left side of the rightmost patches in  $X_1$ , however the right side has been modulated to match the interior patches in  $X_2$  using local padding which is provided from the middle patches of  $X_2$ . The same process can be applied to the second dimension, however this time the outer patches will be the horizontal bottom patches and will be regenerated to match the new image. This iterative process can be repeated in the two dimensions to generate images of infinite sizes while maintaining consistency between the patches and avoiding visible seams or artefacts. This approach requires storing a fraction of the feature maps in the middle patches of  $X_j$  to be used for local padding in  $X_{j+1}$  patches. However, in our implementation, storing these values of each image is less than 0.13 MB for patches of size  $h \times w = 64 \times 64$  or  $h \times w = 128 \times 128$ .

The presented scaling approach utilizes GPU resources efficiently while maintaining a constant memory footprint, as only a fraction of the GPU memory is required for generating the small-size patches, even when moving up to very large sizes. This is in contrast to other methods that scale with GPU memory, which can quickly become memory-intensive and limit the size of the textures that can be generated. Table 1 presents a comparison between the developed method and other related GANs work based on GPU scalability, the use of coordinates, the use of zero-padding, and whether they are trainable on single images. This expansion process cannot be applied directly to traditional texture GANs methods [9, 10] as they use zero-padding and do not generate images in parts.

Table 1: Comparison of various GANs methods focusing on GPU scalability, coordinate-free implementation, padding-free processing, and suitability for generating single images.

GANs Method	Constant GPU Scalability	Coordinate-free	Avoids zero-padding	Single-image
PSGAN [10]	✗	✓	✗	✓
SinGANs [21]	✗	✓	✗	✓
Adversarial Expansions [11]	✗	✓	✗	✓
LocoGAN [22]	✗	✗	✗	✓
ALIS [16]	✓	✗	✗	✗
InfinityGAN [15]	✓	✗	✓	✗
Ours	✓	✓	✓	✓

## 4 Experiments

### 4.1 Datasets

The training examples used in the experiments are texture images obtained mostly from the supplementary materials in [11]<sup>1</sup>. We selected the images such that they are homogeneous and stationary in nature. This is because the developed patch-by-patch approach is designed to generate images in patches and cannot handle such non-stationary patterns. Additionally, we obtained a satellite image from Google Earth<sup>2</sup>, which was used to generate the samples in figure 3, as well as a binary-channelized geological image [30]. The code is available [https://github.com/ai4netzero/Infinite\\_Texture\\_GANs](https://github.com/ai4netzero/Infinite_Texture_GANs).

### 4.2 Results

Firstly, we show the visual quality of the proposed method by presenting some generated textures. Figure 4 shows some sample texture images generated by the trained models. As can be observed, the method generates textures with fine details and smooth transitions between patches, resulting in visually pleasing images. Additionally, the generated textures preserve the overall structure and characteristics of the original textures.




In figure 5, we compared the proposed approach with different texture generating methods: PSGAN [10], Adversarial Expansion [11], and SinGAN [21] – based on the GPU memory required to generate texture images at various sizes. While the proposed method maintains a constant GPU memory requirement regardless of the generated image size, the other methods exhibit a direct and proportional growth in GPU memory consumption relative to the image size.

Table 2 presents a comparison of SIFID (Single Image FID) [21], a metric used to assess the quality and fidelity of generated images produced by GANs based on a single image. SIFID values are calculated for PSGAN [10], SinGAN [21] and our method based on the evaluation of three distinct images. Each row of the table is dedicated to a specific image, with the first column showcasing

<sup>1</sup>The examples can be found at: [https://github.com/jessemelpolio/non-stationary\\_texture\\_syn](https://github.com/jessemelpolio/non-stationary_texture_syn)

<sup>2</sup><https://earthview.withgoogle.com/chile-1151>

Table 2: Comparison of SIFID Values for Different methods (lower is better).

Image	PSGAN	SinGAN	Ours
	0.22	0.27	<b>0.04</b>
	<b>0.08</b>	0.76	0.2
	0.12	0.69	<b>0.09</b>

the visual representation of the image. As reported, the quality of generated texture images by our method is comparable to those generated by PSGAN and SinGAN.

The proposed method has the ability to introduce local changes while maintaining consistency throughout the rest of the image. This is achieved by modulating the corresponding parts in the spatial  $z$  input and spatial map  $M$ , which allows for precise control over the synthesis of localized variations in the texture. This can be seen in figure 6, which depicts two examples of texture images generated using the proposed method. In the first row, we observe how the method has introduced local changes in the form of flowers variations in the bottom right corner, while keeping the overall structure of the texture intact. Similarly, in the second example, the method has introduced localized changes, in top left corner, in the form of new texture patterns while keeping the rest of the image consistent. These results demonstrate the effectiveness of the proposed method in generating high-quality texture images with localized variations that enhance their visual appeal and realism.

To evaluate the effectiveness of the method, we conducted an ablation study. We performed two experiments, in each one we ablate one of the two main components in the proposed method: a) the local padding and replacing it with conventional zero-padding and b) stochastic spatial modulation and replacing it with the standard batch normalization [31]. Figure 7 shows examples of images generated using zero-padding instead of local padding. In this figure, when zero-padding is utilized, noticeable seams and discontinuities become apparent between patches, disrupting the visual coherency of the generated output. These seams and discontinuities arise due to the inherent nature of zero-padding, where the padding values are set to zero, leading to abrupt transitions at the boundary

between patches. In contrast, the utilization of local padding in the generator effectively mitigates these issues by replacing the zero-padding with padding derived from neighbouring content. Consequently, the output generated, as shown in figure 4, with local padding exhibits smoother and more seamless transitions between patches, resulting in a visually consistent and coherent image.

In order to test the effectiveness of the stochastic spatial modulation, we studied texture images that required long-term alignment. For this particular cases, the  $z$  input is kept constant for all patches belonging to the same image and is identical for all spatial positions, thereby serving as a global shared information. The map  $M$ , on the other hand, became the only source of variations. On the other hand, in the experiment with batch-normalization (BN), the local input was concatenated with the global input within the  $z$  vector, similar to [22]. Figure 8 demonstrates that SSM consistently outperformed the alternative method, where the images generated using SSM exhibited significantly better global alignment compared to those generated using batch-normalization. This suggests that disentangling the shared global information from the local stochastic element and introducing it at all scales using SSM effectively preserved the long-range alignment required for those texture images. We also observed that using SSM, particularly in the case of bricks as shown in the middle column of figure 8, resulted in a non-uniform thickness of the bricks. This could be due to the use of replicate padding in the outer patches and local padding in the interior patches.

We also studied the effect of having a fully convolutional generator instead of a traditional generator that uses a fully connected layer followed by convolutional layers similar to [5]. The results in figure 9 show that the fully convolutional generator is able to generate diverse and visually appealing textures, while the generator with a fully connected layer suffers from spatial mode collapse, producing less varied textures.

The proposed method for generating texture images of arbitrary size represents a promising scalable solution in the field of texture synthesis. However, there are several limitations to be considered. One limitation is associated with generating aligned textures (e.g., bricks), the model fails to maintain the alignment in the long-range and introduces artefacts in the form of non-uniform patches. Another significant limitation of the method is its inability to effectively handle non-stationary textures. Non-stationary textures, characterized by spatial variations in the spatial domain, cannot be effectively captured by a model that generates small-size patches independently and assembles them to form larger images.

## 5 Conclusion

In conclusion, this paper presented a novel approach for synthesizing stationary textures of infinite sizes using a patch-by-patch generation technique trained on a single texture image. The proposed method addresses the limitation of memory scalability and the generation of large arbitrary-size textures, which have

challenged previous methods. By generating images in patches and incorporating the novel local padding, the model successfully generated visually appealing texture images with intricate details and seamless transitions between patches. In addition, the use of spatial stochastic modulation in the generator improves the alignments of patterns in certain textures. Infinite-size textures can be synthesized by assembling the generated small-size patches in a scalable way without a proportional growth in GPU memory. Nevertheless, this approach has its limitations, including the challenge of dealing with non-stationary textures and preserving alignments without introducing artefacts in images characterized by global features, which could be explored in future studies.

## 6 Acknowledgment

The first author thanks TotalEnergies for the financial support. The authors acknowledge TotalEnergies for authorizing the publication of this paper.

## References

- [1] A. A. Efros and T. K. Leung, “Texture synthesis by non-parametric sampling,” in *Proceedings of the seventh IEEE international conference on computer vision*, vol. 2, pp. 1033–1038, IEEE, 1999.
- [2] A. A. Efros and W. T. Freeman, “Image quilting for texture synthesis and transfer,” in *Proceedings of the 28th annual conference on Computer graphics and interactive techniques*, pp. 341–346, 2001.
- [3] I. Goodfellow, J. Pouget-Abadie, M. Mirza, B. Xu, D. Warde-Farley, S. Ozair, A. Courville, and Y. Bengio, “Generative adversarial nets,” in *Advances in neural information processing systems*, pp. 2672–2680, 2014.
- [4] T. Karras, S. Laine, and T. Aila, “A style-based generator architecture for generative adversarial networks,” in *Proceedings of the IEEE/CVF conference on computer vision and pattern recognition*, pp. 4401–4410, 2019.
- [5] A. Brock, J. Donahue, and K. Simonyan, “Large scale GAN training for high fidelity natural image synthesis,” *arXiv preprint arXiv:1809.11096*, 2018.
- [6] J.-Y. Zhu, T. Park, P. Isola, and A. A. Efros, “Unpaired image-to-image translation using cycle-consistent adversarial networks,” in *Proceedings of the IEEE international conference on computer vision*, pp. 2223–2232, 2017.
- [7] C. Ledig, L. Theis, F. Huszár, J. Caballero, A. Cunningham, A. Acosta, A. Aitken, A. Tejani, J. Totz, Z. Wang, *et al.*, “Photo-realistic single image super-resolution using a generative adversarial network,” in *Proceedings of*

- the IEEE conference on computer vision and pattern recognition*, pp. 4681–4690, 2017.
- [8] D. Pathak, P. Krahenbuhl, J. Donahue, T. Darrell, and A. A. Efros, “Context encoders: Feature learning by inpainting,” in *Proceedings of the IEEE conference on computer vision and pattern recognition*, pp. 2536–2544, 2016.
  - [9] N. Jetchev, U. Bergmann, and R. Vollgraf, “Texture synthesis with spatial generative adversarial networks,” *arXiv preprint arXiv:1611.08207*, 2016.
  - [10] U. Bergmann, N. Jetchev, and R. Vollgraf, “Learning texture manifolds with the periodic spatial gan,” *arXiv preprint arXiv:1705.06566*, 2017.
  - [11] Y. Zhou, Z. Zhu, X. Bai, D. Lischinski, D. Cohen-Or, and H. Huang, “Non-stationary texture synthesis by adversarial expansion,” *arXiv preprint arXiv:1805.04487*, 2018.
  - [12] T. Karras, S. Laine, M. Aittala, J. Hellsten, J. Lehtinen, and T. Aila, “Analyzing and improving the image quality of stylegan,” in *Proceedings of the IEEE/CVF conference on computer vision and pattern recognition*, pp. 8110–8119, 2020.
  - [13] T. Karras, M. Aittala, S. Laine, E. Härkönen, J. Hellsten, J. Lehtinen, and T. Aila, “Alias-free generative adversarial networks,” *Advances in Neural Information Processing Systems*, vol. 34, 2021.
  - [14] C. H. Lin, C.-C. Chang, Y.-S. Chen, D.-C. Juan, W. Wei, and H.-T. Chen, “Coco-gan: Generation by parts via conditional coordinating,” in *Proceedings of the IEEE/CVF international conference on computer vision*, pp. 4512–4521, 2019.
  - [15] C. H. Lin, H.-Y. Lee, Y.-C. Cheng, S. Tulyakov, and M.-H. Yang, “Infinitygan: Towards infinite-pixel image synthesis,” *arXiv preprint arXiv:2104.03963*, 2021.
  - [16] I. Skorokhodov, G. Sotnikov, and M. Elhoseiny, “Aligning latent and image spaces to connect the unconnectable,” in *Proceedings of the IEEE/CVF International Conference on Computer Vision*, pp. 14144–14153, 2021.
  - [17] A. Radford, L. Metz, and S. Chintala, “Unsupervised representation learning with deep convolutional generative adversarial networks,” *arXiv preprint arXiv:1511.06434*, 2015.
  - [18] M. Arjovsky, S. Chintala, and L. Bottou, “Wasserstein GAN,” *arXiv preprint arXiv:1701.07875*, 2017.
  - [19] I. Gulrajani, F. Ahmed, M. Arjovsky, V. Dumoulin, and A. C. Courville, “Improved training of Wasserstein GANs,” in *Advances in neural information processing systems*, pp. 5767–5777, 2017.

- [20] T. Miyato, T. Kataoka, M. Koyama, and Y. Yoshida, “Spectral normalization for generative adversarial networks,” *arXiv preprint arXiv:1802.05957*, 2018.
- [21] T. R. Shaham, T. Dekel, and T. Michaeli, “Singan: Learning a generative model from a single natural image,” in *Proceedings of the IEEE/CVF International Conference on Computer Vision*, pp. 4570–4580, 2019.
- [22] L. Struski, S. Knop, P. Spurek, W. Daniec, and J. Tabor, “Locogan—locally convolutional gan,” *Computer Vision and Image Understanding*, vol. 221, p. 103462, 2022.
- [23] A. Frühstück, I. Alhashim, and P. Wonka, “Tilegan: synthesis of large-scale non-homogeneous textures,” *ACM Transactions on Graphics (ToG)*, vol. 38, no. 4, pp. 1–11, 2019.
- [24] R. Liu, J. Lehman, P. Molino, F. Petroski Such, E. Frank, A. Sergeev, and J. Yosinski, “An intriguing failing of convolutional neural networks and the coordconv solution,” *Advances in neural information processing systems*, vol. 31, 2018.
- [25] X. Huang and S. Belongie, “Arbitrary style transfer in real-time with adaptive instance normalization,” in *Proceedings of the IEEE international conference on computer vision*, pp. 1501–1510, 2017.
- [26] V. Dumoulin, J. Shlens, and M. Kudlur, “A learned representation for artistic style,” *arXiv preprint arXiv:1610.07629*, 2016.
- [27] D. Ulyanov, A. Vedaldi, and V. Lempitsky, “Instance normalization: The missing ingredient for fast stylization,” *arXiv preprint arXiv:1607.08022*, 2016.
- [28] T. Park, M.-Y. Liu, T.-C. Wang, and J.-Y. Zhu, “Semantic image synthesis with spatially-adaptive normalization,” in *Proceedings of the IEEE Conference on Computer Vision and Pattern Recognition*, pp. 2337–2346, 2019.
- [29] P. Isola, J.-Y. Zhu, T. Zhou, and A. A. Efros, “Image-to-image translation with conditional adversarial networks,” in *Proceedings of the IEEE conference on computer vision and pattern recognition*, pp. 1125–1134, 2017.
- [30] S. Strebelle, “Conditional simulation of complex geological structures using multiple-point statistics,” *Mathematical geology*, vol. 34, no. 1, pp. 1–21, 2002.
- [31] S. Ioffe and C. Szegedy, “Batch normalization: Accelerating deep network training by reducing internal covariate shift,” in *International conference on machine learning*, pp. 448–456, pmlr, 2015.

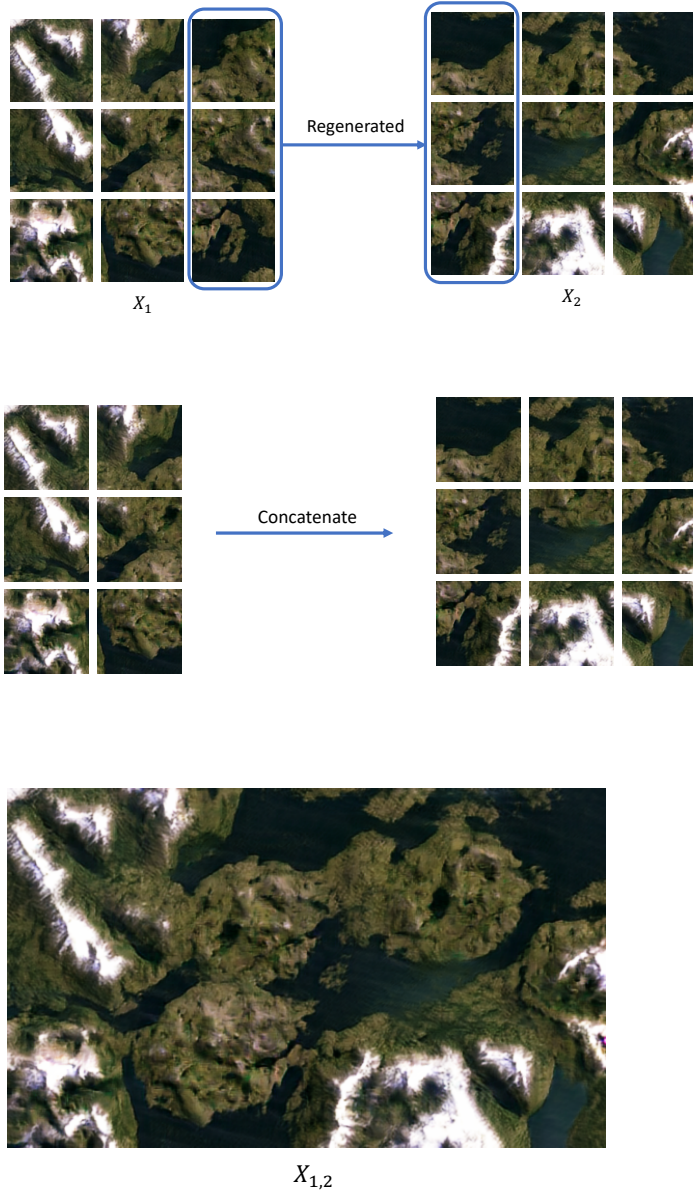


Figure 3: Scaling in the horizontal direction: (Top) Two images  $X_1$  and  $X_2$ , each composed of  $3 \times 3$  generated patches, where the rightmost patches in  $X_1$  are regenerated to match the interior patches of  $X_2$  (Middle) the rightmost patches in  $X_1$  are removed since they have been regenerated (Bottom) the final image  $X_{1,2}$  composed of  $3 \times 5$  patches assembled after dropping the outer patches in  $X_1$  and concatenating the rest of  $X_1$  with  $X_2$ .



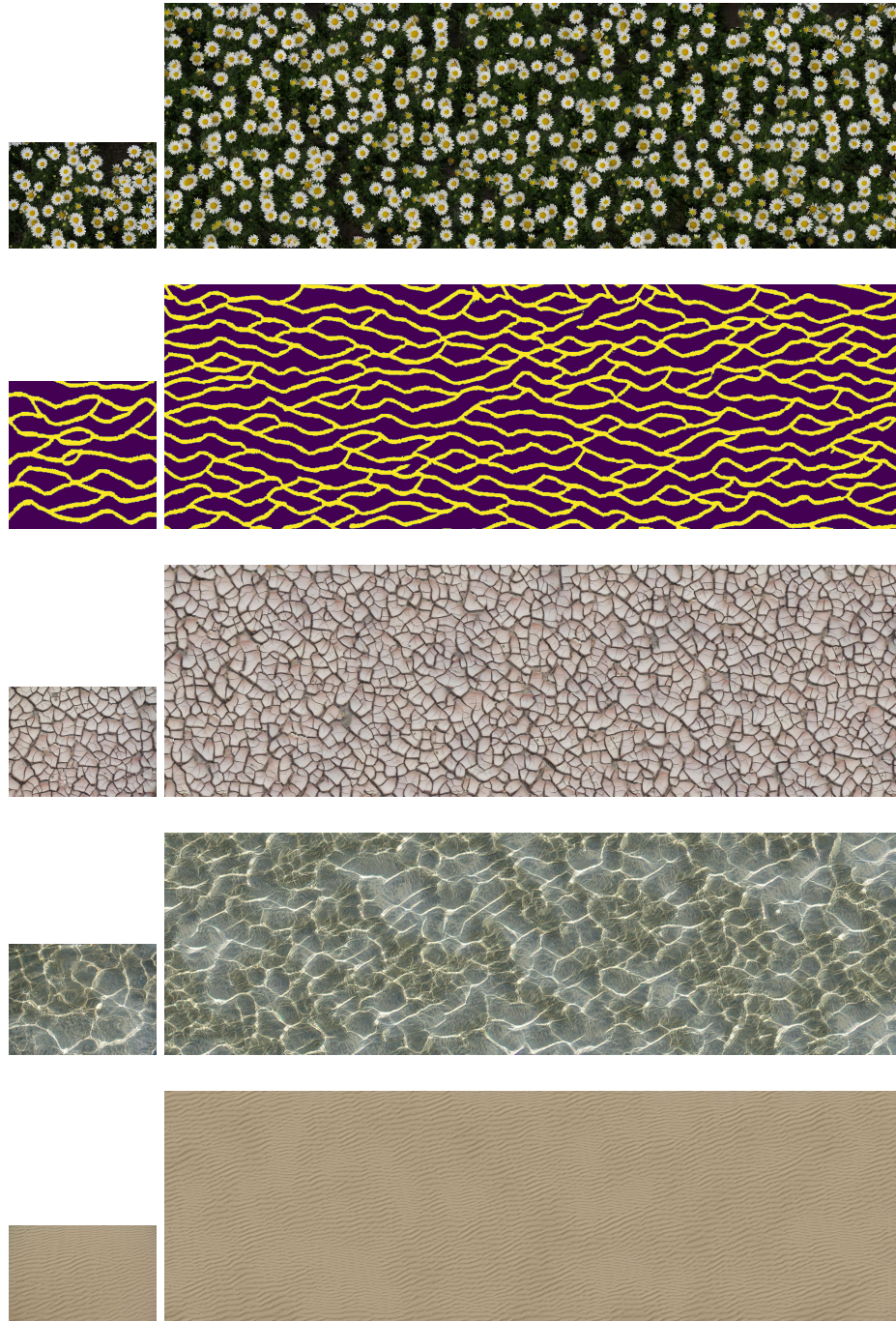


Figure 4: Examples of texture images generated by the proposed method (right column) given the source texture (left column).

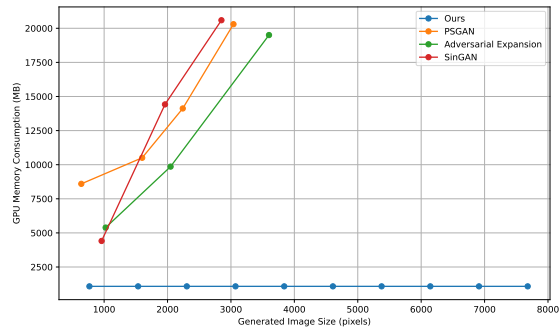


Figure 5: Comparison between the proposed method, PSGAN [10], adversarial expansion [11], and SinGAN [21] based on the GPU memory required to generate images with different sizes. The evaluation was conducted on a single GPU with 24GB of RAM. Notably, the proposed patch-by-patch method maintains a constant GPU memory requirement across all sizes, in contrast to the other methods, where the required GPU memory increases with the size of the generated image.

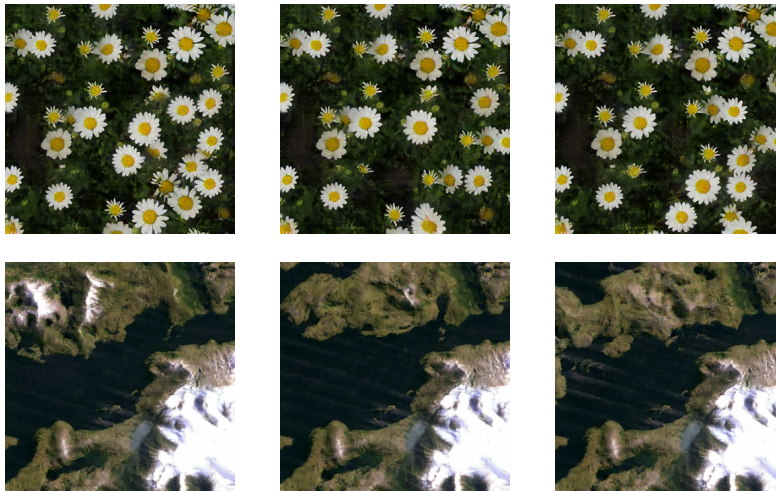


Figure 6: Illustration of two examples of texture images generated using the proposed method with GANs. The images showcase how the method can introduce local changes while maintaining consistency throughout the rest of the texture. The images show texture variations in the bottom right corner (first row) and the top left corner (second row), while the rest of the image is kept almost the same. Notice that part of the change is broadcasted in the middle patches to match the introduced change.



Figure 7: Two examples of texture images generated using zero-padding instead of local padding. The images illustrate how zero-padding leads to visible seaming artefacts between the patches.

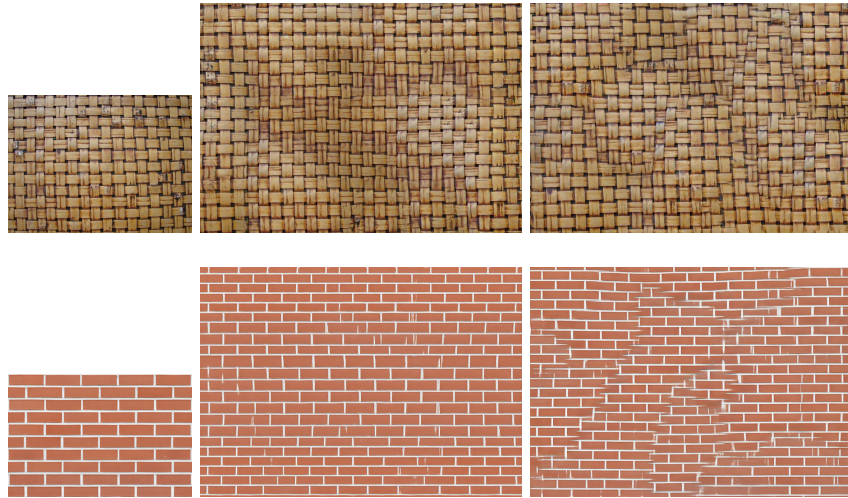


Figure 8: Comparisons of generating larger textures from the source images (first column) between two methods: Stochastic Spatial Modulation (SSM) as the only source of stochasticity (second column), and a combination of local and global inputs within the  $z$  vector with Batch Normalization (BN) (third column). The results demonstrate that using SSM better preserves the long-term alignment in the generated textures.

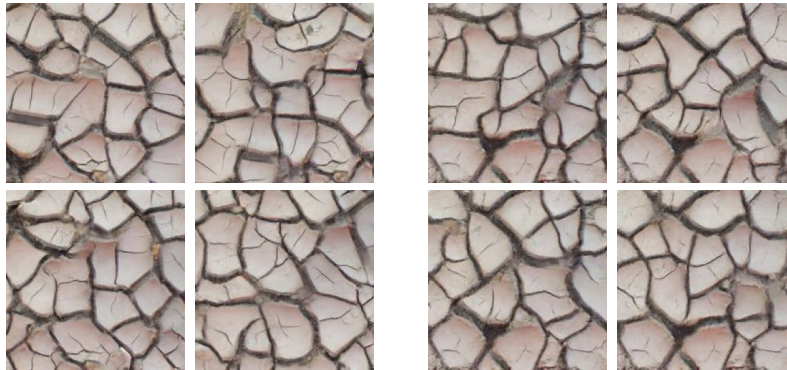


Figure 9: Comparison of texture generated using a fully convolutional generator (left) versus a generator with a fully connected layer (right). The fully convolutional generator demonstrates diverse texture samples, whereas the generator with a fully connected layer suffers from spatial mode collapse, producing less varied textures, as evidenced in areas such as the bottom left corners.